

# The variations of VOCs based on the policy change of Omicron in traffic-hub city Zhengzhou

Bowen Zhang<sup>1,3</sup>, Dong Zhang<sup>2,3</sup>, Zhe Dong<sup>2,3</sup>, Xinshuai Song<sup>1,3</sup>, Ruiqin Zhang<sup>1,3</sup>,  
Xiao Li<sup>1,3,\*</sup>

<sup>1</sup>School of Ecology and Environment, Zhengzhou University, Zhengzhou 450001,  
China

<sup>2</sup>College of Chemistry, Zhengzhou University, Zhengzhou 450001, China

<sup>3</sup>Institute of Environmental Sciences, Zhengzhou University, Zhengzhou 450001,  
China

Correspondence to: Xiao Li, E-mail address: [lixiao9060@zzu.edu.cn](mailto:lixiao9060@zzu.edu.cn)

**Abstract:** Online volatile organic compounds (VOCs) were monitored before and after the Omicron policy change at an urban site in polluted Zhengzhou from December 1, 2022, to January 31, 2023. The characteristics and sources of VOCs were investigated. The daily mean concentrations of PM<sub>2.5</sub> and total VOCs (TVOCs) ranged from 53.5 to 239.4  $\mu\text{g}/\text{m}^3$  and 15.6 to 57.1 ppbv, respectively, with mean values of  $111.5 \pm 45.1 \mu\text{g}/\text{m}^3$  and  $36.1 \pm 21.0$  ppbv, respectively, throughout the period. Two severe pollution events (designated as Case 1 and Case 2) were identified in accordance with the National Ambient Air Quality Standards (NAAQS) (China's National Ambient Air Quality Standards (NAAQS) from 2012). Case 1 (December 5 to December 10, PM<sub>2.5</sub> daily mean = 142.5  $\mu\text{g}/\text{m}^3$ ) and Case 2 (January 1 to January 8, PM<sub>2.5</sub> daily mean = 181.5  $\mu\text{g}/\text{m}^3$ ) occurred during the infection period (when the policy of "full nucleic acid screening measures" was in effect) and the recovery period (after the policy was cancelled), respectively. The PM<sub>2.5</sub> and TVOCs values for Case 2 are, respectively, 1.3 and 1.8 times higher than those for Case 1. The results of the positive matrix factor modeling demonstrated that the primary source of volatile organic compounds (VOCs) during the observation period was industrial emissions, which constituted 32% of the total VOCs, followed by vehicle emissions (27%) and combustion (21%). In Case 1, industrial emissions constituted the primary source of VOCs, accounting for 32% of the total VOCs. In contrast, in Case 2, the contribution of vehicular emission sources increased to 33% and became the primary source of VOCs. The secondary organic aerosol formation potential for Case 1 and Case 2 were found to be 37.6  $\mu\text{g}/\text{m}^3$  and 65.6  $\mu\text{g}/\text{m}^3$ , respectively. In Case 1, the largest contribution of SOAP from industrial sources accounted for the majority (63%, 23.8  $\mu\text{g}/\text{m}^3$ ), followed by vehicular sources (18%).

34 After the end of the epidemic and the resumption of productive activities in the society,  
35 the difference in the proportion of SOA generated from various sources decreased. Most  
36 of the SOAP came from solvent use and fuel evaporation sources, accounting for 32%  
37 (20.9  $\mu\text{g}/\text{m}^3$ ) and 26% (16.8  $\text{go}/\text{m}^3$ ), respectively. On days with minimal pollution,  
38 industrial sources and solvent use remain the main contributors to SOA formation.  
39 Therefore, regulation of emissions from industry, solvent-using industries and motor  
40 vehicles need to be prioritized to control the  $\text{PM}_{2.5}$  pollution problem.

41

42 **Keywords: Volatile organic compounds; Pollution episode; Source apportionment; Positive**  
43 **Matrix Factorization model; Secondary organic aerosol formation potential;**

## 44 **1. Introduction**

45 Volatile organic compounds (VOCs) in the atmosphere have high reactivity and  
46 can react with nitrogen oxides (NO<sub>x</sub>) to form a series of secondary pollutants such as  
47 ozone (O<sub>3</sub>) and secondary organic aerosol (SOA), resulting in regional air pollution (Li  
48 et al., 2019; Hui et al., 2020). The problem of O<sub>3</sub> pollution has been plaguing major  
49 urban agglomerations in China (Zheng et al., 2010; Li et al., 2014; Wang et al., 2017).  
50 SOA is an important component of fine particulate matter (PM<sub>2.5</sub>) and contributes  
51 significantly to haze pollution (Liu et al., 2019). PM<sub>2.5</sub> remains the most significant air  
52 pollutant in many Chinese cities for years (Shao et al., 2016; Wu et al., 2016). In  
53 addition, VOCs, represented by the benzene homologues, can cause damage to kidneys,  
54 liver, and nervous system of humans when they enter the body (Zhang et al., 2018).

55 Studies have shown that the most common VOC components in China are alkanes,  
56 olefins, aromatic hydrocarbons, oxygenated VOCs (OVOCs), and halogenated  
57 hydrocarbons, among which alkanes are the most abundant species (Liu et al., 2020;  
58 Zhang et al., 2021a). VOCs in the atmosphere have a wide range of sources, and VOCs  
59 in different regions are affected by multiple factors such as local geography, climate,  
60 and human activities (Mu et al., 2023; Zou et al., 2023). The above reasons lead to  
61 significant regional and seasonal differences in the characteristics of VOCs (Song et al.,  
62 2021). For example, the annual average concentration of VOCs in the coastal  
63 background area of the Pearl River Delta is 9.3 ppbv. The seasonal variation trend of  
64 VOCs is high in autumn and winter and low in summer (Yun et al., 2021). In contrast,  
65 the average VOC concentration in autumn and winter in Beijing was  $22.6 \pm 12.6$  ppbv,  
66 and the VOC concentration in the winter heating period was twice that in the autumn  
67 non-heating period (Niu et al., 2022).

68 Moreover, the sources of VOC components in different regions are also related to  
69 the local industrial structure and living habits. In rural areas of North China Plain in  
70 winter, it is found that the SOA formation potential (SOAP) of VOCs under low NO<sub>x</sub>  
71 conditions is significantly higher than that under high NO<sub>x</sub> conditions, and the increase  
72 of aromatic hydrocarbon emissions caused by coal combustion is the main reason for  
73 the higher SOAP in winter (Zhang et al., 2020). Li et al. (2022) found that the average  
74 increased concentration of acetylene was 4.8 times from autumn to winter in the  
75 Guanzhong Plain, indicating that fuel combustion during the heating period in winter  
76 has a significant impact on the composition of VOCs. In contrast, continuous

77 observations conducted by Zhou et al. (2022) in the suburbs of Dongguan in summer  
78 found that industrial solvent usage, liquefied petroleum gas (LPG) and oil and gas  
79 volatilization were the main sources of VOCs. The results highlighted a wide variation  
80 of characteristics, sources and chemical reactions of VOCs in the atmosphere thus it is  
81 necessary to investigate VOCs in different cities when formulating control measures.

82 Zhengzhou, as the capital of Henan Province, is an important transportation hub  
83 and economic center in the Central Plains region. Zhengzhou is currently facing  
84 significant air pollution problems, with the Air Quality Index at the bottom of the  
85 national ranking of 168 cities for many years. In January 2023, for example, the number  
86 of polluted days with PM<sub>2.5</sub> as the primary pollutant was 17, and the daily average value  
87 of PM<sub>2.5</sub> reached a maximum of 298 µg/m<sup>3</sup>  
88 ([https://www.aqistudy.cn/historydata/daydata.php?city=%E9%83%91%E5%B7%9E](https://www.aqistudy.cn/historydata/daydata.php?city=%E9%83%91%E5%B7%9E&month=202301)  
89 &month=202301, Accessed Jan 2024), which is almost 300% higher than the Chinese  
90 daily average standard (grade II, 75 µg/m<sup>3</sup>). The studies of VOCs were carried out in  
91 Zhengzhou in recent years, which focused on the characteristics and sources of VOCs  
92 during pollution episodes (Lai et al., 2024) or before the coronavirus epidemic outbreak  
93 (Li et al., 2020; Zhang et al., 2021b). While some atmospheric VOCs studies involving  
94 the impact of Covid-19 lockdown have been performed in India (Singh et al., 2023a),  
95 in China (e.g., Pei et al., 2022; Jensen et al., 2023; Zuo et al., 2024), or with respect to  
96 toluene, benzene, m/p-xylene and ethylbenzene only (e.g., Sahu et al., 2022; Singh et  
97 al., 2023b), a gap persisted in the investigation of VOCs due to the impact of  
98 abolishment of China's zero-policy. Furthermore, some studies have discussed the  
99 impact of changes in human production activities on air pollution during and after the  
100 outbreak of the coronavirus disease (e.g., Ma et al., 2022; Jiang et al., 2023; Song et al.,  
101 2023), but as mentioned earlier, only a few studies with in-depth exploration of the  
102 changes in VOCs and none dealing with ending the zero-Covid policy during Omicron  
103 variant infection period.

104 In this study, we conducted continuous online observations of VOCs during the  
105 polluted winter season at an urban site in Zhengzhou. The study covered the period  
106 following the removal of lockdown measures. We focused on pollution events when the  
107 daily average PM<sub>2.5</sub> concentration exceeded 75 µg/m<sup>3</sup> (China's Class II standard) for  
108 more than three consecutive days. Days with PM<sub>2.5</sub> concentrations below 35 µg/m<sup>3</sup>  
109 (China's Class I standard) were classified as clean days. During this period, China lifted  
110 zero-COVID strategies, announcing the '10 measures' for optimizing COVID-19 rules

111 on December 7, 2022 ([http://www.news.cn/politics/2022-12/07/c\\_1129189285.htm](http://www.news.cn/politics/2022-12/07/c_1129189285.htm),  
112 Accessed Jan 2024). Zhengzhou's epidemic prevention and control measures changed  
113 with the issuance of Circular No. 163 on December 4, 2022, which allowed the  
114 reopening of closed public places. As a result, movement within Zhengzhou increased  
115 and social production resumed. Our research specifically examines the period  
116 dominated by the COVID-19 Omicron variant. where they demonstrate notable  
117 differences from the early virus strains (i.e., original SARS-CoV-2 virus and Delta) in  
118 terms of geographical transmission, the scale of the infected population, and symptom  
119 manifestation (Petersen et al., 2022; Merino et al., 2023).

120 After the quarantine policy was lifted, people basically rested at home due to  
121 infection or fear of infection with Omicron. The resumption of normal production and  
122 life depends on herd immunization. This outbreak event is the longest in duration and  
123 the largest in number of infections since the 2020 outbreak of the novel coronavirus in  
124 Zhengzhou. It would be beneficial to investigate the impact of this event on emissions  
125 related to transportation and industrial production. This change is worth exploring in  
126 terms of its impact on transportation and industrial production emissions. Therefore,  
127 the characteristics and variations of VOCs during different periods were investigated to  
128 assess their impact on the formation of SOA and to provide data support for future  
129 pollution control policies in Zhengzhou.

130

## 131 **2. Materials and methods**

### 132 **2.1 Sample collection and Chemical analysis**

133 The online VOCs observation station is located on the roof of the Zhengzhou  
134 Environmental Protection Monitoring Center, which is in the urban area. The sampling  
135 site is close to main roads on three sides (150 m away from Funiu Road on the east side,  
136 200 m away from Qinling Road on the west side, and connected to Zhongyuan Road  
137 on the south side), and surrounded by residential areas and commercial areas without  
138 other large nearby stationary sources. The sampling period for this study was from  
139 December 1, 2022, to January 31, 2023, and serious PM<sub>2.5</sub> pollution in Zhengzhou was  
140 of frequent occurrence during December and January.  
141 ([https://www.aqistudy.cn/historydata/monthdata.php?city=%e9%83%91%e5%b7%9e](https://www.aqistudy.cn/historydata/monthdata.php?city=%e9%83%91%e5%b7%9e#:~:text=%E7%94%9F%E5%91%BD%E6%9D%A5%E6%BA%90%E8%87%AA%E7%84%B6%EF%BC%8C%E5%81%A5)  
142 [#:~:text=%E7%94%9F%E5%91%BD%E6%9D%A5%E6%BA%90%E8%87%AA%](https://www.aqistudy.cn/historydata/monthdata.php?city=%e9%83%91%e5%b7%9e#:~:text=%E7%94%9F%E5%91%BD%E6%9D%A5%E6%BA%90%E8%87%AA%E7%84%B6%EF%BC%8C%E5%81%A5)  
143 [E7%84%B6%EF%BC%8C%E5%81%A5](https://www.aqistudy.cn/historydata/monthdata.php?city=%e9%83%91%e5%b7%9e#:~:text=%E7%94%9F%E5%91%BD%E6%9D%A5%E6%BA%90%E8%87%AA%E7%84%B6%EF%BC%8C%E5%81%A5)). Apart from a brief occurrence of rain and  
144 snow on December 25, the sampling days were either sunny or cloudy. The wind speed  
145 (WS), temperature (Temp) and relative humidity (RH) during this period were  $1.3 \pm 0.9$   
146 m/s,  $5.3 \pm 3.2$  °C and  $38.9 \pm 19.0\%$ ), respectively, similar to the values observed in  
147 previous years in Zhengzhou. It is interesting to point out that the sampling period in  
148 the present study covered the entire infection period of Omicron in Zhengzhou,  
149 including the phase of surge in infected population (Infection period, from 2022.12.01  
150 to 2022.12.31) and restoration of production and livelihood phase (Recovery period,  
151 from 2023.1.1 to 2023.1.31 in 2023) (Fig. S1, Chinese Center for Disease Control and  
152 Prevention, 2023).

153 The VOCs were measured hourly using a GC-FID/MS (TH-PKU 300 b, Wuhan  
154 Tianhong Instruments Co., China). The instrument TH-PKU300b includes electronic  
155 refrigeration ultra-low temperature pre-concentration sampling system, analysis system  
156 and system control software. The ambient VOCs in the first 5 minutes of each hour  
157 were collected by the sampling system and then entered the concentration system.  
158 Under low temperature conditions, the VOCs samples collected were frozen in the  
159 capillary capture column, and then quickly heated and resolved, so that the compounds  
160 entered the analysis system. After separation by chromatographic column, the  
161 compounds were monitored by FID and MS detectors. During the detection process,  
162 the atmospheric samples collected undergo analysis through two distinct pathways. C2-  
163 C5 hydrocarbons are analyzed using FID, while C5-C12 hydrocarbons, halocarbons,

164 and OVOCs are analyzed with a MS detector. After excluding species with missing data  
165 exceeding 10%, the detected volatile organic compounds include 29 alkanes, 11 alkenes,  
166 17 aromatics, 35 halocarbons, 12 OVOCs, 1 alkyne (acetylene), and 1 sulfide (CS<sub>2</sub>)  
167 with a total of 106 compounds. A detailed description of the instrumentation can be  
168 found in our previous study (Zhang et al., 2021b; Shi et al., 2022; Zhang et al., 2024).

169 The instrument was calibrated per week to ensure the accuracy of VOCs by  
170 injecting standard gases with a five-point calibration curve. The detection limit of C2-  
171 C5 hydrocarbons ranges from 0.007 to 0.099 ppbv, other hydrocarbons are 0.004–0.045  
172 ppbv, halogenated hydrocarbons 0.009-0.099 ppbv, OVOCs and other compounds of  
173 0.006–0.095 ppbv. Thirty-two of the monitored VOCs had over 90% observed data  
174 greater than the detection limit, and 34 had more than 50% observed data greater than  
175 the detection limit.

176 Simultaneous observations at the same site were also carried out for particulate  
177 matter (PM<sub>2.5</sub>, PM<sub>10</sub>), other trace gases (carbon monoxide (CO), O<sub>3</sub>, nitric oxide (NO),  
178 nitrogen dioxide (NO<sub>2</sub>)), and meteorological data (Temperature, RH, WS, and wind  
179 direction (WD)) based on 1 h resolution.

## 180 **2.2 Positive Matrix Factorization (PMF) model**

181 EPA PMF5.0 model was used for the quantitative source analysis of VOCs (Norris  
182 et al., 2014). The principles and methods have been described in detail in previous  
183 studies (Mozaffar et al., 2020; Zhang et al., 2021b). The decomposition of the PMF  
184 mass balance equations is simplified as follows (Norris et al., 2014):

185

$$186 \quad x_{ij} = \sum_{k=1}^p g_{ik} f_{kj} + e_{ij} \quad (1)$$

187

188 where  $x_{ij}$  is the mass concentration of species  $j$  measured in sample  $i$ ;  $g_{ik}$  is the  
189 contribution of factor  $k$  to the sample  $i$ ;  $f_{kj}$  represents the content of the  $j$ th species in  
190 factor  $k$ ;  $e_{ij}$  is the residual of species  $j$  in sample  $i$ ;  $p$  represents the number of factors.

191 The fitting objective of the PMF model is to minimize the function  $Q$  to obtain the  
192 factor contributions and contours. The formula for  $Q$  is given in Eq. (2):

193

194 
$$Q = \sum_{i=1}^n \sum_{j=1}^m \left[ \frac{x_{ij} - \sum_{k=1}^p g_{ik} f_{kj}}{u_{ij}} \right]^2 \quad (2)$$

195

196 where  $n$  and  $m$  denote the number of samples and VOC species, respectively.

197 Concentrations and uncertainty data are required for the PMF model. In this study,  
 198 the median concentration of a given species is used to replace missing values with an  
 199 uncertainty of four times of the median values; data less than the Method Detection  
 200 Limit (MDL) were replaced with half the MDL, with an uncertainty of 5/6 of the MDL;  
 201 and the uncertainty for values greater than the MDL was calculated using Eq. (3). In  
 202 Eq. (3),  $EF$  is error fraction, expressed as the precision of VOCs species, and the setting  
 203 range can be adjusted from 5 to 20% according to the concentration difference (Buzcu  
 204 et al., 2006; Song et al., 2007); and  $c_{ij}$  is the concentration of species  $j$  in sample  $i$ :

205 
$$U_{ij} = \sqrt{(EF \times c_{ij})^2 + (0.5 \times MDL)^2} \quad (3)$$

206 when the concentration of VOCs in the species is less than the value of the  
 207 detection limit  $U_{ij}$  is calculated using Eq. (4):

208 
$$U_{ij} = \left(\frac{5}{6}\right) MDL \quad (4)$$

209 VOC species and concentration input into PMF were carefully selected to ensure  
 210 the accuracy of the PMF results. Species were excluded when over 25% of the samples  
 211 were missing or concentrations values were below the MDL (Gao et al., 2018); VOCs  
 212 with a short lifetime in the atmosphere were also excluded unless they are source-  
 213 relative species (Zhang et al., 2014; Shao et al., 2016). After that, retained VOC species  
 214 were categorized according to the signal-to-noise ratio (S/N) with  $S/N < 0.2$  species  
 215 categorized as bad,  $0.2 < S/N < 2$  species categorized as weak; and  $S/N > 2$  species  
 216 categorized as strong (Shao et al., 2016).

217 We used displacement of factor elements (DISP) to assess PMF modelling  
 218 uncertainty (for a description, see Paatero et al. (2014)).  $Q$  was less than 1% and no  
 219 swaps occurred for the small est  $dQ^{\max}$  in DISP.  $F_{\text{peak}}$  values from -2 to 2 were tested  
 220 to explore the rotational stability of the solutions.  $Q_{\text{true}}/Q_{\text{exp}}$  is lowest when  $F_{\text{peak}} = 0$ ,  
 221 so we chose the PMF results for that case (Fig. S2a). After examining 3-8 factors, 20  
 222 base runs with 5 factors eventually selected to represent final result. We provide an  
 223 explanation of factor selection in the supplementary materials. Fig. S2(b) includes  
 224  $Q_{\text{true}}/Q_{\text{exp}}$ ,  $Q_{\text{robust}}/Q_{\text{exp}}$  for factors 3-8. The slopes of these two ratios in changed at five



225 factors, and we found that five factors were more realistic after repeated comparisons  
226 of the results at four, five and six factors.

## 227 **2.3 SOA generation potential**

228 The contributions of VOC species to SOAP were calculated based on the toluene  
229 weighted mass contributions (TMC) method (Derwent et al., 2010). The methodology  
230 for calculating SOAP is as follows:

231

$$232 \text{SOAPF}_i = \frac{\text{VOCs component } i \text{ to SOA mass concentration increments}}{\text{Toluene to SOA mass concentration increment}} \times 100 \quad (5)$$

233

234  $\text{SOAPF}_i$  for each VOC is taken from the literature (Derwent et al., 2010). The  
235 SOAP was estimated by multiplying the  $\text{SOAPF}_i$  value by the concentration of  
236 individual VOC species. The SOAP calculations through each VOC are as follows:

237

$$238 \text{SOAP} = \sum E_i \times \text{SOAPF}_i \quad (6)$$

239  $E_i$  is the concentration of species  $i$ .

240

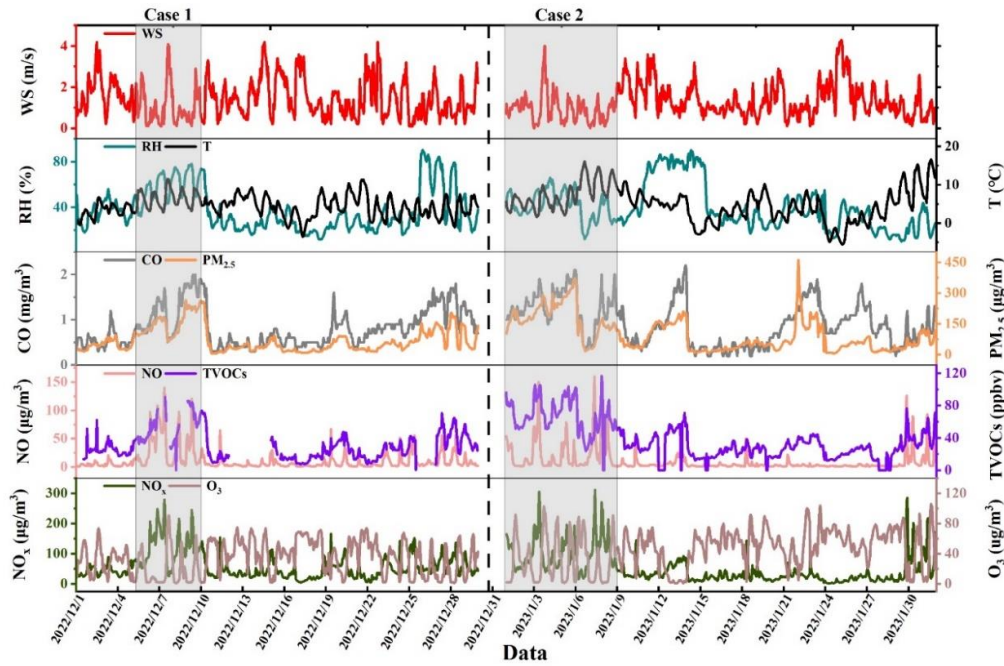
## 241 **3. Results and discussion**

### 242 **3.1 Overview of variation in pollutants and meteorological** 243 **parameters**

244 Figure 1 shows the time series of meteorological parameters, TVOCs, O<sub>3</sub>, NO<sub>x</sub>,  
245 SO<sub>2</sub>, CO and PM<sub>2.5</sub> during the observed periods. Low WS and Temperature were found  
246 with an average value of  $1.3 \pm 0.6$  m/s and  $5.0 \pm 2.5$  °C, respectively, during the entire  
247 period, comparable with observations at the same site in 2021 (Lai et al., 2024). A total  
248 of 62 days of valid data was acquired with the daily average concentration of PM<sub>2.5</sub>  
249 ranging from 53 to 239  $\mu\text{g}/\text{m}^3$ , with the average value of  $111 \pm 45$   $\mu\text{g}/\text{m}^3$ . The  
250 concentration of TVOCs ranged from 15.6 to 57.1 ppbv with an average of  $36.1 \pm 21.0$   
251 ppbv, higher than the same period in last year ( $27.9 \pm 12.7$  ppbv, Lai et al., 2024).  
252 During the observation period, the average values of T, WS and RH were  $5.0 \pm 2.5$  °C,  
253  $1.3 \pm 0.6$  m/s and  $38.9 \pm 16.7\%$ , respectively.

254 Previous studies have shown that meteorological factors such as low WS, high RH,

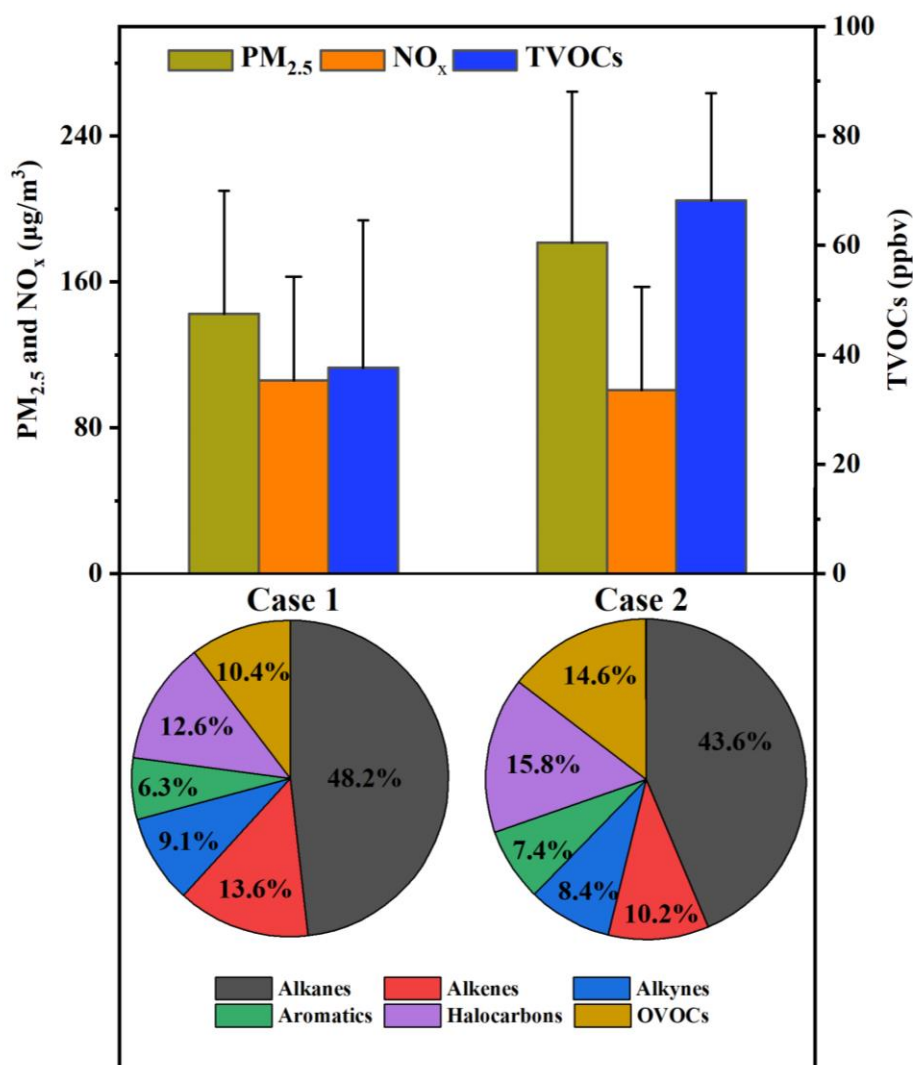
255 and low precipitation are responsible for the increase in PM<sub>2.5</sub> pollution in Zhengzhou  
256 in winter (Duan et al., 2019). Our analysis of the correlation between different  
257 pollutants and meteorological conditions during the pollution period showed that  
258 PM<sub>2.5</sub>, TVOCs and NO<sub>x</sub> were positively correlated with relative humidity (Fig. S3),  
259 which is consistent with the results of some previous studies (Wang et al., 2019). Yu  
260 et al. (2018) identified RH and WS as the most influential meteorological conditions  
261 of PM<sub>2.5</sub> during winter. Their findings revealed a positive correlation between hourly  
262 PM<sub>2.5</sub> concentrations and RH ( $r = 0.84, p < 0.01$ ) and a negative correlation between  
263 PM<sub>2.5</sub> concentrations and WS ( $r = -0.62, p < 0.01$ ). The WS and RH between the  
264 infection and recovery periods were similar in this study which were largely  
265 considered to be of the same type of weather (Yu et al., 2018). However, the mean  
266 PM<sub>2.5</sub> concentration during the recovery period was found to be 1.6 times higher than  
267 that observed during the infection period. Furthermore, the concentrations of other  
268 pollutants (including SO<sub>2</sub>, NO<sub>2</sub>, CO, and O<sub>3</sub>) exhibited analogous trends during the  
269 infection and recovery periods. The concentration of TVOCs during the recovery  
270 period was 1.2 times higher than that during the infection period, exhibiting a  
271 significant upward trend following the resumption of production. It is notable that WS,  
272 which is only 0.3 m/s higher in Case 1 than in Case 2, and RH, which is 13% higher  
273 in Case 1 than in Case 2, were relatively stable, while the concentration of pollutants  
274 is significantly higher in Case 2 than in Case 1. This is presumably attributable to the  
275 resumption of production activities in Case 2, which resulted in a notable increase in  
276 emissions. Decreased trends of air pollutants were found in other studies before and  
277 after the outbreak of the novel coronavirus (COVID-19) in early 2020 (Qi et al., 2021;  
278 Wang et al., 2021).



279

280 Fig. 1. Time series of WS, T, RH, CO, PM<sub>2.5</sub>, NO, TVOCs, NO<sub>x</sub> and O<sub>3</sub> during the observation  
 281 period.

282 The shadow section in Fig. 1 represents two haze pollution events during the  
 283 monitoring period. A pollution event is determined when the daily average  
 284 concentration of PM<sub>2.5</sub> exceeds 75 µg/m<sup>3</sup> (China's II-level standard) for at least three  
 285 consecutive days. Case 1 (December 5 to December 10 with daily average PM<sub>2.5</sub> =  
 286 142.5 µg/m<sup>3</sup>) and Case 2 (January 1 to January 8 with daily average PM<sub>2.5</sub> = 181.5  
 287 µg/m<sup>3</sup>) were selected as they represent the pollution events in infection and recovery  
 288 periods, respectively, due to their long duration and high pollution levels. Any day with  
 289 a PM<sub>2.5</sub> concentration lower than 35 µg/m<sup>3</sup> (China's I-level standard) is considered as  
 290 Clean day.



291  
 292 Fig. 2. The concentration of PM<sub>2.5</sub>, NO<sub>x</sub>, TVOCs and the composition ratio of VOCs in Case 1 and  
 293 Case 2.

294 As for the two representative pollution processes (Case 1 during the infection  
 295 period and Case 2 during the recovery period), the concentration of TVOCs in Case 1  
 296 and Case 2 were  $48.4 \pm 20.4$  and  $67.6 \pm 19.6$  ppbv (Fig. 2), respectively, increased by  
 297 63% and 188% compared with values during clean days. The average concentrations  
 298 of PM<sub>2.5</sub> and TVOCs during Case 2 were 1.3 and 1.8 times the values in Case 1. The  
 299 highest volume contributions of alkanes were found both in Case 1 (48%) and Case 2  
 300 (44%), consistent with the results in the Yangtze River Delta region (36-43%, Liu et al.,  
 301 2023). While alkenes exhibited higher volume percentages of 13% in Case 1, followed  
 302 by halogenated hydrocarbon (12%) and OVOCs (10%). Higher volume percentages of  
 303 alkanes and alkenes in Case 1 were similar to the results in the gasoline evaporation  
 304 site in winter (Niu et al., 2022). Equivalent volume contribution of halogenated  
 305 hydrocarbon and OVOCs (15%) were found in Case 2, followed by alkenes (10%).

306 Although aromatic hydrocarbons have the lowest volumetric contribution (6% in Case  
 307 1 and 7% in Case 2), they show the largest increase from clean days to pollution.

308 Table 1 The average concentrations of meteorological parameters and pollutants during different  
 309 processes.

Category	Entire process (2022.12.1- 2023.1.31)	Infection period (2022.12.1- 2022.12.31)	Recovery period (2023.1.1- 2023.1.31)	Case 1 (2022.12.5- 2022.12.10)	Case 2 (2023.1.1- 2023.1.8)	Clean Days
	N = 62 days	N = 31 days	N = 31 days	N = 6 days	N = 8 days	N = 8 days
WS (m/s)	1.3 ± 0.6	1.4 ± 0.6	1.3 ± 0.6	1.2 ± 0.9	0.9 ± 0.7	1.4 ± 0.8
T (°C)	5.0 ± 2.5	4.7 ± 1.7	5.4 ± 3.1	6.1 ± 2.2	7.4 ± 3.5	4.1 ± 3.0
RH (%)	38.9 ± 16.7	37.6 ± 15.5	40.2 ± 18.2	55.7 ± 14.7	42.0 ± 12.1	29.5 ± 18.1
TVOCs (ppbv)	36.1 ± 21.0	31.9 ± 18.1	39.8 ± 22.4	37.6 ± 27.0	68.2 ± 19.6	22.7 ± 11.1
SO <sub>2</sub> (µg/m <sup>3</sup> )	11.4 ± 2.7	10.2 ± 2.8	12.7 ± 2.3	11.0 ± 3.7	16.2 ± 6.1	6.5 ± 2.5
NO <sub>2</sub> (µg/m <sup>3</sup> )	47.2 ± 10.0	46.8 ± 8.6	47.8 ± 11.7	62.7 ± 20.5	65.0 ± 21.3	20.8 ± 15.9
CO (mg/m <sup>3</sup> )	0.9 ± 0.2	0.8 ± 0.2	1.1 ± 0.2	1.2 ± 0.5	1.3 ± 0.4	0.5 ± 0.2
O <sub>3</sub> (µg/m <sup>3</sup> )	34.9 ± 6.0	31.1 ± 4.5	39.0 ± 4.6	21.8 ± 23.7	32.5 ± 29.6	52.6 ± 18.4
PM <sub>2.5</sub> (µg/m <sup>3</sup> )	111.5 ± 45.1	86.6 ± 34.6	138.3 ± 39.6	142.5 ± 67.4	181.5 ± 82.7	23.8 ± 16.8

310 Table 2 Concentration of VOC species during different processes (ppbv).

Category	Entire process	Infection period	Recovery period	Case 1	Case 2	Clean days
TVOCs	36.1 ± 21.0	31.9 ± 18.1	39.8 ± 22.4	48.4 ± 20.4	67.6 ± 19.6	17.5 ± 9.5
alkanes	16.8 ± 9.2	15.0 ± 8.4	18.4 ± 9.5	23.1 ± 10.0	29.5 ± 8.4	9.2 ± 5.6
alkenes	4.1 ± 2.7	3.8 ± 2.6	4.4 ± 2.7	6.5 ± 2.9	7.0 ± 2.6	1.7 ± 1.3
alkynes	3.1 ± 2.0	2.7 ± 1.7	3.4 ± 2.1	4.3 ± 2.0	5.8 ± 1.9	1.3 ± 0.8
aromatics	2.1 ± 2.0	1.8 ± 1.5	2.3 ± 2.2	3.0 ± 1.8	4.9 ± 2.8	0.7 ± 0.5
halogenated hydrocarbon	5.4 ± 3.3	4.4 ± 2.3	6.2 ± 3.8	6.0 ± 1.9	10.7 ± 3.6	2.7 ± 1.4
OVOCs	4.6 ± 3.2	3.5 ± 2.7	5.1 ± 3.5	5.0 ± 2.4	9.7 ± 2.8	1.9 ± 1.1

### 311 3.2 Source Analysis of VOCs

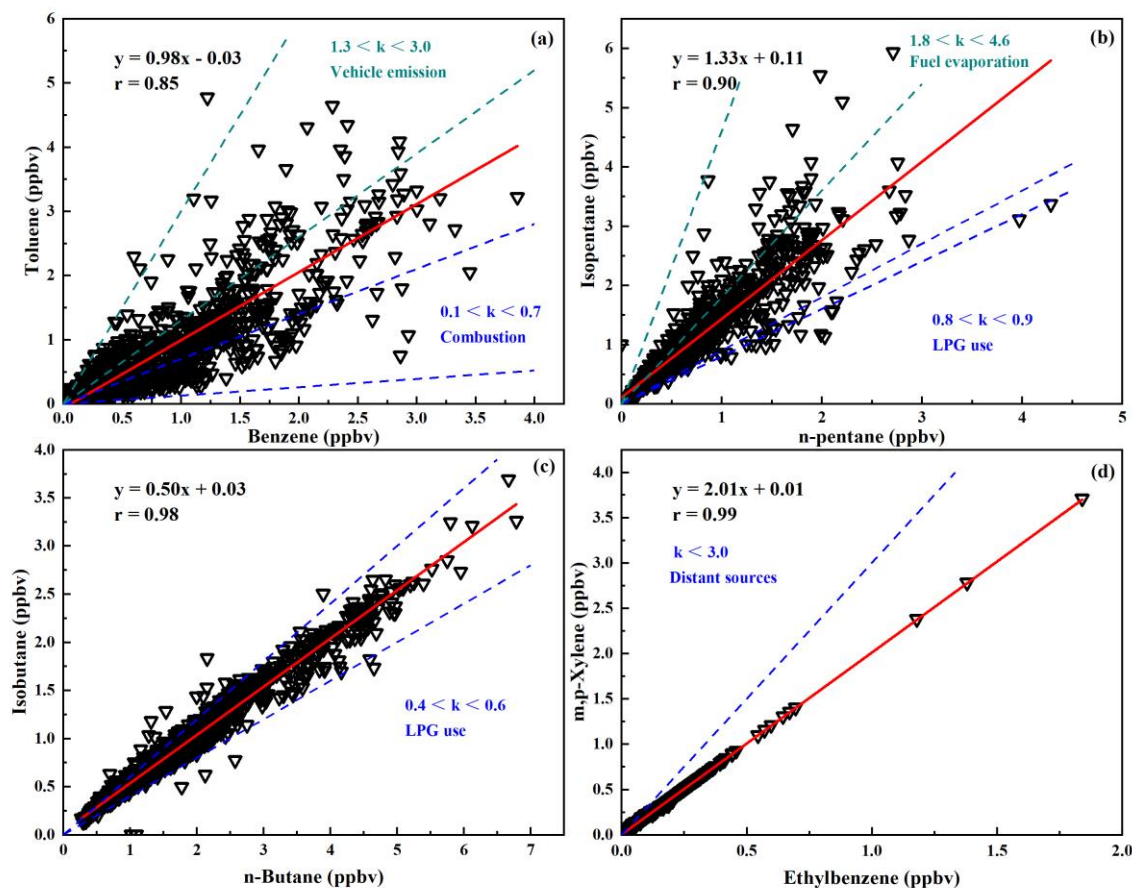
312 Specific VOC ratios can be used for initial source identification of VOCs and  
 313 determination of photochemical ages of air masses (Monod et al., 2001; An et al., 2014;  
 314 Li et al., 2019). In this study, the ratios of toluene/benzene (T/B), isopentane/n-pentane,  
 315 isobutane/n-butane, and m/p-xylene/ethylbenzene (X/E) were selected to initially  
 316 identify the potential sources of VOCs (Fig. 3). Concentrations of selected pollutants  
 317 and ratios used are shown in Table S1.

318 The toluene-to-benzene ratio (T/B ratio) was widely used to assess the relative  
319 importance of different sources. Specifically, T/B ratio with a value of 1.3-3.0 was  
320 observed in vehicle emissions for vehicles with different fuel types (Schauer et al., 2002;  
321 Wang et al., 2015). The reported T/B ratio for combustion processes was between 0.13  
322 and 0.7 (Li et al., 2011; Wang et al., 2014). The mean value of T/B ratio for the entire  
323 period was 1.0, with the majority of the data (99%) falling between 0.1 and 3.0 and  
324 concentrated within the 0.7-1.3 range (49%). This suggests that both traffic emissions  
325 and combustion are significant sources of VOCs.

326 The isopentane/n-pentane concentration ratios of 0.6-0.8 represent mainly coal  
327 combustion emissions, ratios of 0.8-0.9 represent LPG emissions, 2.2-3.8 represent  
328 vehicle exhaust emissions, and 1.8-4.6 represent fuel evaporation (Conner et al., 1995;  
329 Liu et al., 2008; Li et al., 2019). The sources of isopentane and n-pentane in this study  
330 were intricate and multifaceted. The mean isopentane/n-pentane ratio was 1.4, with the  
331 majority of data points (99%) falling within the range of 0.1-4.6, with a notable  
332 concentration in the 0.8 to 1.8 interval. This indicates that pentane is influenced by a  
333 combination of emissions from LPG and fuel evaporation.

334 Isobutane/n-butane concentration ratios of 0.2-0.3 represent vehicle emissions,  
335 0.4-0.6 represent LPG usage, and 0.6-1.0 represent natural gas emissions (Russo et al.,  
336 2010; Zheng et al., 2018). The mean isobutane/n-butane ratio in this study was 0.5, with  
337 the majority of data points (99%) falling within the 0.4-0.6 range, indicating that VOCs  
338 at the observation sites were significantly influenced by the use of LPG. (Shao et al.,  
339 2016; Zeng et al., 2023).

340 The ratio of X/E can be used to infer the photochemical age of the air mass. X/E  
341 ratios around 2.5-2.9 are typical of urban areas, indicating that VOCs are mainly from  
342 the urban area (fresh air mass) (Kumar et al., 2018). When this ratio is significantly  
343 lower than 3.0, it indicates that VOCs are mainly transported from distant sources  
344 (aging air masses) (Kumar et al., 2018). The average X/E value in this study was 2.0  
345 (Fig. 3(d)), indicating low photochemical activity and aging of the air mass at the  
346 observation site. Potential source analyses also indicate that air masses are affected by  
347 long-range transport (Fig. S4).



348

349

Fig. 3. Correlation analysis between specific VOC species.

350

Figure 4 shows the chemical profiles of individual VOCs resolved by the PMF model during the entire observation period. These five factors eventually selected as potential sources for the observed VOCs are: (1) Fuel evaporation; (2) Solvent usage; (3) Vehicular emission; (4) Industrial source; and (5) Combustion. These 5 factors have been commonly reported before, e.g., in Shijiazhuang, northern China (Guan et al, 2023) and in Beijing (Cui et al., 2022).

356

Alkanes of C4-C6 substances were predominant in factor 1, including 2-methylpentane, 3-methylpentane, isobutane, n-butane, isopentane and n-pentane from oil and gas (Xiong et al., 2020). Fig. S5 shows that emissions from this source peak at midday, when fuel volatilization is high, The CPF plot shows that south-east is the dominant direction at wind speeds of less than 2 m/s (Fig. 5a). Therefore, factor 1 was identified as the source of oil and gas volatilization.

362

The contribution of benzene, toluene, methylene chloride, 1,2-dichloroethane and ethyl acetate was high in factor 2. It has been shown that benzene, toluene, ethylbenzene, and xylene is an important component in the use of solvents (Li et al., 2015); methylene

364

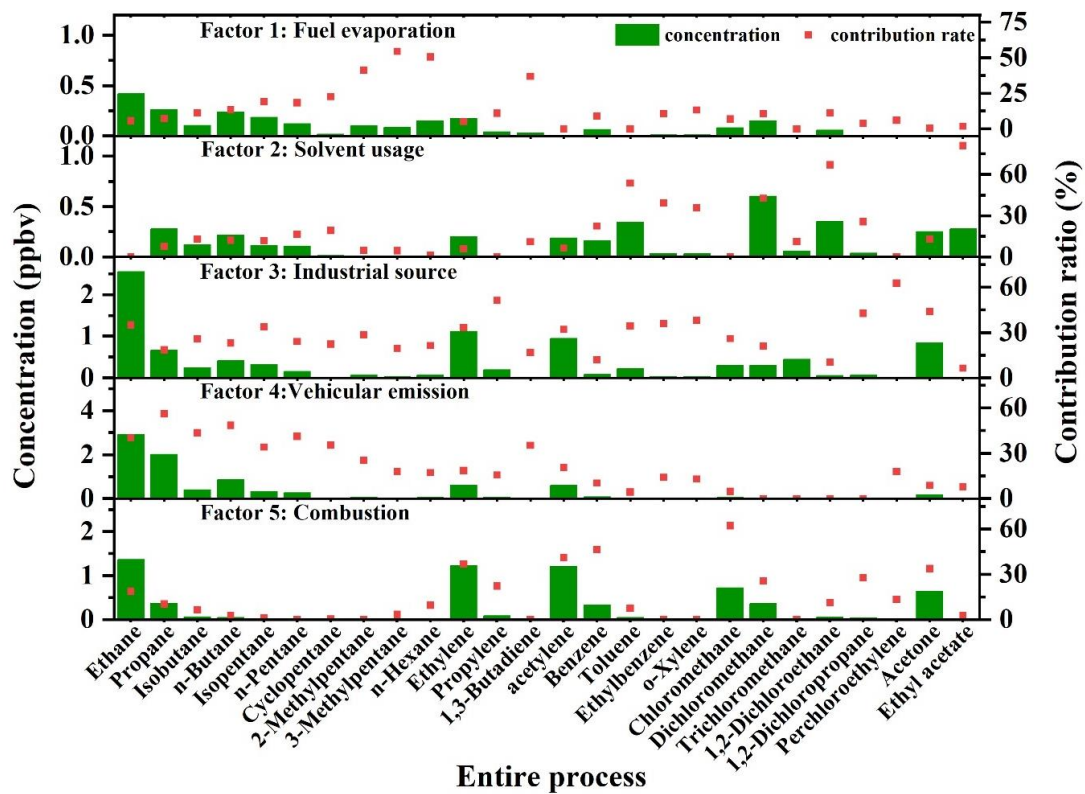
365 chloride is often used as a chemical solvent, while esters are mostly used as industrial  
366 solvents or adhesives (Li et al., 2015). Factor 2 is determined to be solvent usage source.  
367 The CPF plot shows that due east is the main emission direction at wind speeds less  
368 than 2 m/s and southeast is the main source at wind speeds greater than 2 m/s (Fig. 5b).

369 Factor 3 contains predominantly C3-C8 alkanes, olefins and alkynes, and  
370 relatively high concentrations of benzene. These substances are usually emitted by  
371 industrial processes (Shao et al., 2016), so Factor 4 is defined as an industrial source.  
372 The CPF plots indicate that a local source at low wind speeds is the dominant sources  
373 (Fig. 5c).

374 Factor 4 is characterized by relatively high levels of C2-C6 low-carbon alkanes  
375 (ethane, propane, isopentane, n-pentane, isobutane and n-butane), olefins (ethylene and  
376 propylene), and benzene and toluene, which are important automotive exhaust tracers  
377 (Song et al., 2021; Zhang et al., 2021b). Ethylene and propylene are important  
378 components derived from vehicle-related activities. Previous studies of VOCs in  
379 Zhengzhou have shown a high percentage of VOCs emitted from gasoline vehicles,  
380 with the main source of alkanes being on-road mobile sources (Bai et al., 2020). The  
381 daily variation of this source in Fig. S5 shows a bimodal trend, with peaks occurring in  
382 the morning and evening peaks of traffic, consistent with motor vehicle emissions. Fig.  
383 5d shows that this source is mainly from the west where wind speeds are below 2 m/s,  
384 and in this direction, there are a number of urban arterial roads with high traffic volumes.  
385 Therefore, factor 4 was defined as vehicular emission source.

386 The highest contribution to factor 5 is chloromethane (62%). Benzene (46%) and  
387 acetylene (41%) also contribute highly to factor 5. Chloromethane is the key tracer for  
388 biomass combustion and acetylene is the key tracer for coal combustion (Xiong et al.,  
389 2020). Therefore, factor 5 is defined as a combustion source. The CPF plot shows that  
390 at wind speeds below 2 m/s, the north-east direction is the dominant source direction  
391 (Fig. 5e).

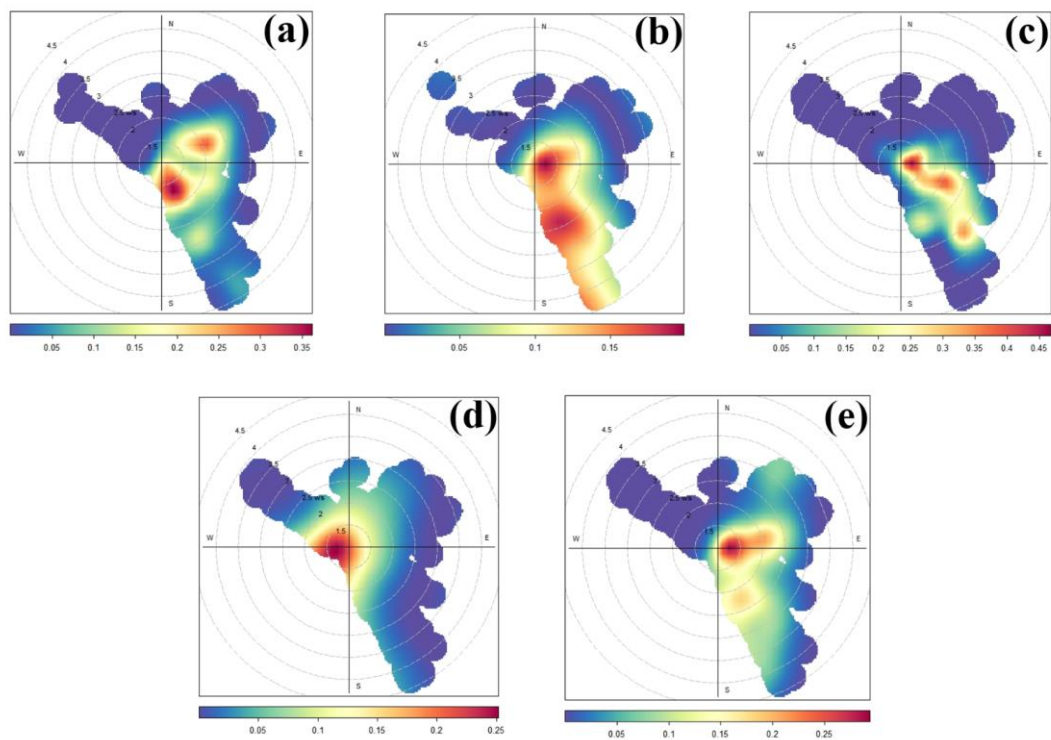




392

393

Fig. 4. Concentration of VOC species in each factor and contribution to each source.



394

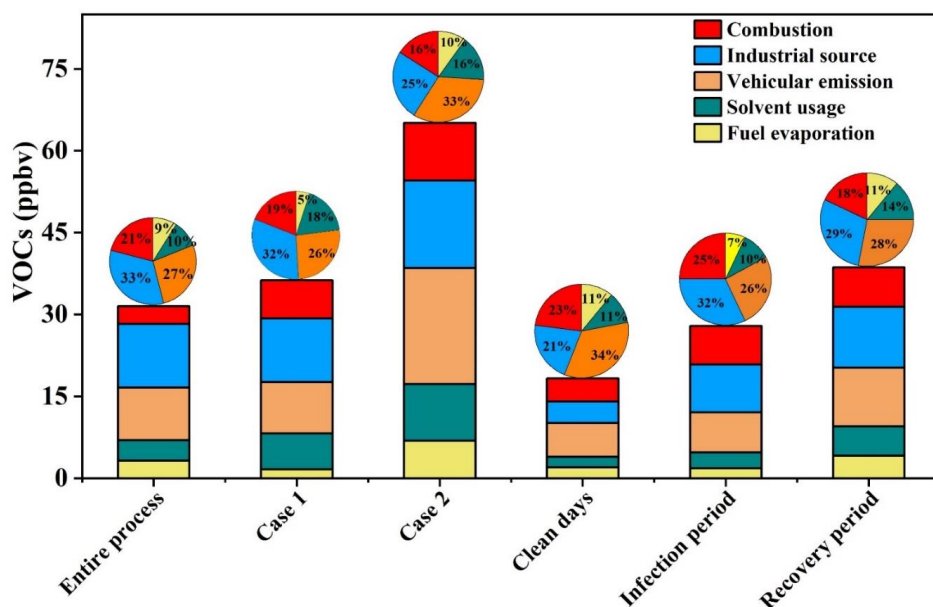
395

Fig. 5. CPF plots of five VOCs sources obtained using the PMF model.

396 Note: a: Fuel evaporation; b: Solvent usage; c: Industrial source; d: Vehicular emission; e:  
 397 Combustion.

398 Fig. S6 compares the differences in PMF source profiles between the Omicron  
 399 infection period and the recovery period, as well as between the pollution day and the  
 400 clean day. We present the concentrations of the five main VOCs in all five factors in  
 401 Table S2. Ethane (vehicular emission), 2-methylpentane (fuel evaporation), benzene  
 402 (industry source), chloromethane (combustion), and ethyl acetate (solvent usage) were  
 403 selected as tracers for five sources. Ethane concentration in Case 2 (5.9 ppbv) is much  
 404 higher than in other processes, and ethane concentration during the recovery period (3.4  
 405 ppbv) is also higher than during the infection period (2.4 ppbv), which may to some  
 406 extent reflect increased vehicular emissions during the recovery period.

407 Concentrations of most species were significantly higher during the recovery  
 408 period than during the infection period. The representative pollution processes in both  
 409 periods showed the same results as well, with a 79% higher concentration of TVOCs in  
 410 Case 2 (65.1 ppbv) compared to Case 1 (36.3 ppbv) (Fig. 6). While in Case 1 industry  
 411 was the dominant source of VOCs, by Case 2 motorized sources reached a  
 412 concentration value of 21.2 ppbv, accounting for 33% of the observed VOCs, and  
 413 became the dominant source of emissions. This is consistent with the fact that people's  
 414 mobility activities have increased after the epidemic has entered the recovery period.  
 415 As a group of VOCs species with the highest concentration share, ethane and propane  
 416 contributed more to the clean days motor vehicle source than other processes, which  
 417 also resulted in a 34% clean days motor vehicle source share.



418

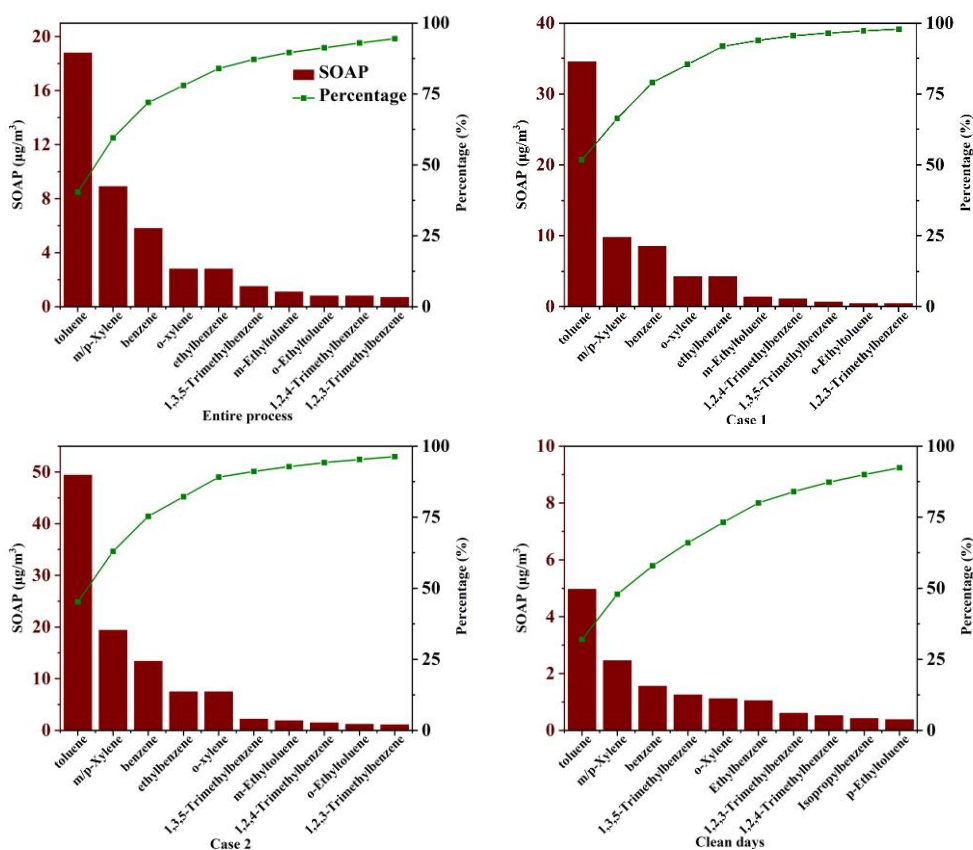
419

Fig. 6. Contribution of each to VOCs for different processes.

### 420 3.3 SOAP

421 VOCs are estimated to contribute about 16–30% or more of PM<sub>2.5</sub> by mass through  
 422 SOA production (Huang et al., 2014). Therefore, by calculating the SOAP value, the  
 423 influence of different sources on PM<sub>2.5</sub> production can be reflected to a certain extent.

424 We have included quantitative analysis for SOAP as well. Fig. 7 shows the SOAP  
 425 concentrations and contribution rates of the top ten species throughout the entire  
 426 process, during two pollution processes, and clean days. The top ten species all reached  
 427 close to 100% of the total SOAP contribution, with Case 1 reaching 98%. In each  
 428 process, the composition of the top ten substances is essentially the same. Aromatic  
 429 hydrocarbons contributed the most, with BTEX always occupying the top five positions  
 430 and toluene the most. The SOAP values of the top ten contributing species for the two  
 431 polluting processes are shown in Tables S3 and S4. Toluene, the highest contributing  
 432 species, reached a SOAP value of 49.4  $\mu\text{g}/\text{m}^3$  in the most polluted Case 2, which was  
 433 3.2 times higher than the SOAP sum of all species on the clean day (15.5  $\mu\text{g}/\text{m}^3$ ). The  
 434 SOAP value for Case 1, which is also a contaminated process, was 67  $\mu\text{g}/\text{m}^3$ , and the  
 435 main species (m/xylene: 9.8  $\mu\text{g}/\text{m}^3$ , benzene: 8.5  $\mu\text{g}/\text{m}^3$ ) including toluene (34.6  $\mu\text{g}/\text{m}^3$ )  
 436 were lower than those for Case 2 (m/xylene: 19.4  $\mu\text{g}/\text{m}^3$ , benzene: 13.4  $\mu\text{g}/\text{m}^3$ ).



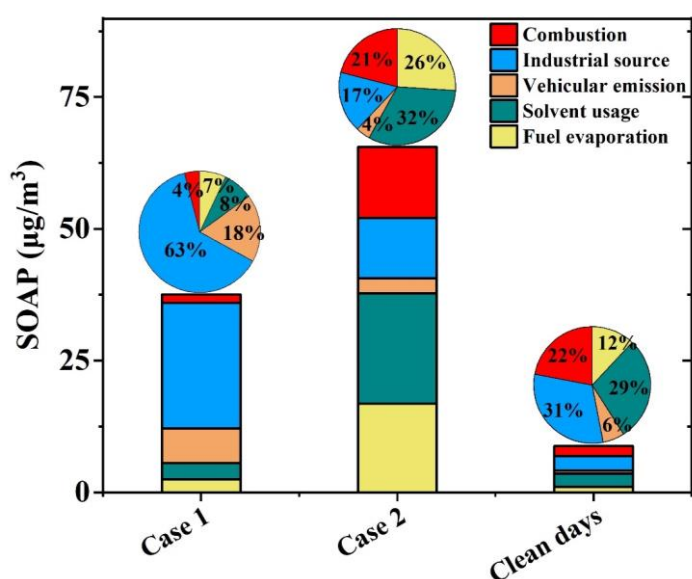
437

438

Fig. 7. SOAP dominant species in different processes

439

440 Figure 8 shows the SOAP calculated after source resolution of the two pollution  
441 processes by PMF for clean days, respectively. In Case 1, industrial source is the  
442 dominant source with a contribution ratio of 63%. In Case 2, the pollution sources  
443 exhibit a more evenly distributed contribution, where the solvent usage and fuel  
444 evaporation sources emerge as the primary contributors to SOAP, with their respective  
445 contribution levels rising to 32% and 26%. Case 1 was during the infection period,  
446 when social activities had not yet returned to normal. In Case 2, when society had  
447 basically returned to normal, the increase in emissions from various sources resulted in  
448 a more balanced distribution of SOAP contributions and caused more severe PM<sub>2.5</sub>  
449 pollution. In addition, a few days before Case 2, the Zhengzhou Municipal People's  
450 Government initiated the Heavy Pollution Weather Level II response (<https://sthjj.zhengzhou.gov.cn/tzgg/7037130.jhtml>) and introduced control measures  
451 for emissions from industrial and mobile sources, which resulted in a significant  
452 reduction of SOAP levels from industrial and motorized sources in Case 2. The clean  
453 day result with a SOAP of 8.8 µg/m<sup>3</sup> also indicates that industrial and solvent usage  
454 sources are the most dominant SOAP sources. The primary sources of aromatic  
455 compounds, which are the most significant contributors to SOAP, are solvent usage and  
456 industrial process emissions. This finding aligns with the results of other studies (Wu  
457 et al., 2017). Consequently, it is imperative to implement measures to reduce PM<sub>2.5</sub>  
458 pollution by regulating emissions from industrial and solvent usage sources.



459

460

461

Fig. 8. SOAP value and contribution ratio of each process

## 462 4. Conclusions

463 Continuous observation of VOCs during the infection of the Omicron epidemic  
464 was carried out at an urban site in polluted Zhengzhou from December 1, 2022, to  
465 January 31, 2023. The daily average concentration of PM<sub>2.5</sub> ranged from 53.5 to 239.4  
466  $\mu\text{g}/\text{m}^3$  with an average value of  $111.5 \pm 45.1 \mu\text{g}/\text{m}^3$  during the whole period. The  
467 concentration of TVOCs ranged from 15.6 to 57.1 ppbv with an average of  $36.1 \pm 21.0$   
468 ppbv, higher than the same period in last year ( $27.9 \pm 12.7$  ppbv, Lai et al., 2024). Two  
469 representative contamination processes were identified (Case 1 during the infection  
470 period and Case 2 during the recovery period). The concentration of TVOCs in Case 1  
471 and Case 2 were  $48.4 \pm 20.4$  and  $67.6 \pm 19.6$  ppbv, respectively, increased by 63% and  
472 188% compared with values during clean days. The average concentrations of PM<sub>2.5</sub>  
473 and TVOCs during Case 2 were 1.3 and 1.8 times of the values in Case 1. This is  
474 consistent with the observed increase in pollutant emissions following the return to  
475 normal social life from the period of Omicron infection. The highest volume  
476 contributions of alkanes were found both in Case 1 (48%) and Case 2 (44%). Though  
477 the volume contribution of aromatics were the lowest (6% in Case 1 and 7% in Case 2),  
478 the highest increase ratio was found from clean days to polluted episodes. Low wind  
479 speed and high humidity were the main meteorological reasons for the occurrence of  
480 pollution. Analyzing the sources of VOCs revealed that VOCs were found to be affected  
481 by a combination of local emissions and regional transport. The primary sources of  
482 atmospheric VOCs in Zhengzhou were identified as industrial emissions (32%), vehicle  
483 emissions (27%), and combustion (21%). Significant discrepancies were observed in  
484 the sources of VOCs between the two pollution processes. In Case 1, industrial  
485 emissions constituted the primary source of VOCs, accounting for 32% of the total  
486 VOC concentration. In contrast, in Case 2, the proportion of vehicle emissions  
487 increased to 33%, representing the primary source of VOCs.

488 A further analysis of the effect of VOCs on SOA generation reveals that aromatic  
489 compounds are the primary contributors to SOAP, with BTEX being the predominant  
490 contributor throughout the period. The SOAP values reached 37.6 and 65.6  $\mu\text{g}/\text{m}^3$  in  
491 Case 1 and Case 2, respectively. In Case 1, the greatest contribution to SOAP was made  
492 by industrial sources (63%, 23.8  $\mu\text{g}/\text{m}^3$ ), while vehicular sources, which constituted the  
493 second most important source, accounted for only 18%. In Case 2, the contribution of  
494 each VOC source was more evenly distributed, with solvent use sources and fuel

495 evaporation sources representing the primary contributors to SOAP, accounting for 32%  
496 (20.9  $\mu\text{g}/\text{m}^3$ ) and 26% (16.8  $\mu\text{g}/\text{m}^3$ ), respectively. The SOAP result for the clean day  
497 was 8.8  $\mu\text{g}/\text{m}^3$ , with industrial sources and solvent use still being the primary  
498 contributors. Therefore, the industrial and solvent use sectors are the predominant  
499 sources of pollutants during this observation. The aforementioned results substantiate  
500 the considerable impact of elevated emissions from all sources on the exacerbation of  
501 pollution following the conclusion of the Omicron infection.

502 **Author contribution:**

503 Bowen Zhang: Data curation, Methodology, Formal analysis, Writing Original Draft.

504 Dong Zhang: Data curation, Formal analysis, Review & Editing.

505 Zhe Dong: Data curation, Formal analysis, Review & Editing.

506 Xinshuai Song: Data curation, Formal analysis.

507 Ruiqin Zhang: Supervision, Writing-Review & Editing, Funding acquisition.

508 Xiao Li: Formal analysis, Investigation, Supervision, Writing-Review & Editing.

509 **Competing interests:**

510 The contact author has declared that none of the authors has any competing interests.

511 **Acknowledgments:**

512 This research was supported by the Natural Science Foundation of Henan Province  
513 (232300421395) and the National Key Research and Development Program of China  
514 (2017YFC0212400).

515 **References**

516 An, J., Zhu, B., Wang, H., Li, Y., Lin, X., and Yang, H.: Characteristics and source  
517 apportionment of VOCs measured in an industrial area of Nanjing, Yangtze River Delta,  
518 China, *Atmospheric Environment*, 97, 206-214,  
519 <https://doi.org/10.1016/j.atmosenv.2014.08.021>, 2014.

520 Bai, L., Lu, X., Yin, S., Zhang, H., Ma, S., Wang, C., Li, Y., and Zhang, R.: A  
521 recent emission inventory of multiple air pollutant, PM<sub>2.5</sub> chemical species and its  
522 spatial-temporal characteristics in central China, *Journal of Cleaner Production*, 269,  
523 122114, <https://doi.org/10.1016/j.jclepro.2020.122114>, 2020.

524 Buzcu, B. and Fraser, M. P.: Source identification and apportionment of volatile

525 organic compounds in Houston, TX, *Atmospheric Environment*, 40, 2385-2400,  
526 <https://doi.org/10.1016/j.atmosenv.2005.12.020>, 2006.

527 Conner, T. L., Lonneman, W. A., Seila, R.L.: Transportation-related volatile  
528 hydrocarbon source profiles measured in atlanta, *Journal of the Air & Waste*  
529 *Management Association*, 45 (5), 383-394,  
530 <https://doi.org/10.1080/10473289.1995.10467370>, 1995.

531 Cui, L., Wu, D., Wang, S., Xu, Q., Hu, R., and Hao, J.: Measurement report:  
532 Ambient volatile organic compound (VOC) pollution in urban Beijing: characteristics,  
533 sources, and implications for pollution control, *Atmospheric Chemistry and Physics*,  
534 22, 11931-11944, <https://doi.org/10.5194/acp-22-11931-2022>, 2022.

535 Derwent, R. G., Jenkin, M. E., Utembe, S. R., Shallcross, D. E., Murrells, T. P.,  
536 and Passant, N. R.: Secondary organic aerosol formation from a large number of  
537 reactive man-made organic compounds, *Science of the Total Environment*, 408, 3374-  
538 3381, <https://doi.org/10.1016/j.scitotenv.2010.04.013>, 2010.

539 Duan, S., Jiang, N., Yang, L., Zhang, R.: Transport Pathways and Potential Sources  
540 of PM<sub>2.5</sub> During the Winter in Zhengzhou, *Environmental Science*, Jan 8;40(1):86-93,  
541 <https://doi.org/10.13227/j.hjlx.201805187>, 2019.

542 Gao, J., Zhang, J., Li, H., Li, L., Xu, L., Zhang, Y., Wang, Z., Wang, X., Zhang,  
543 W., Chen, Y., Cheng, X., Zhang, H., Peng, L., Chai, F., and Wei, Y.: Comparative study  
544 of volatile organic compounds in ambient air using observed mixing ratios and initial  
545 mixing ratios taking chemical loss into account – A case study in a typical urban area  
546 in Beijing, *Science of the Total Environment*, 628-629, 791-804,  
547 <https://doi.org/10.1016/j.scitotenv.2018.01.175>, 2018.

548 Guan, Y., Liu, X., Zheng, Z., Dai, Y., Du, G., Han, J., Hou, L. a., and Duan, E.:  
549 Summer O<sub>3</sub> pollution cycle characteristics and VOCs sources in a central city of  
550 Beijing-Tianjin-Hebei area, China, *Environmental Pollution*, 323, 121293,  
551 <https://doi.org/10.1016/j.envpol.2023.121293>, 2023.

552 Huang, R., Zhang, Y., Bozzetti, C. et al.: High secondary aerosol contribution to p  
553 articulate pollution during haze events in China, *Nature*, 514 (7521), 218–22, <https://doi.org/10.1038/nature13774>, 2014.

555 Hui, L., Liu, X., Tan, Q., Feng, M., An, J., Qu, Y., Zhang, Y., Deng, Y., Zhai, R., a  
556 nd Wang, Z.: VOC characteristics, chemical reactivity and sources in urban Wuhan, ce  
557 ntral China, *Atmospheric Environment*, 224, 117340, <https://doi.org/10.1016/j.atmosenv.2020.117340>, 2020.

559 Jensen, A., Liu, Z., Tan, W., Dix, B., Chen, T., Koss, A., Zhu, L., Li, L., de Gouw,  
560 J.: Measurements of volatile organic compounds during the COVID-19 lockdown in  
561 Changzhou, China, *Geophysical research letters*, 48(20), <https://doi.org/10.1029/2021>  
562 GL095560, 2021.

563 Jiang, N., Hao, X., Hao, Q., Wei, Y., Zhang, Y., Lyu, Z., Zhang, R.: Changes in se  
564 condary inorganic ions in PM<sub>2.5</sub> at different pollution stages before and after COVID-1  
565 9 control, *Environmental Science*, 44(5), 2430-2440, <https://doi.org/10.13227/j.hjcx.2>  
566 02206170, 2023.

567 Kumar, A., Singh, D., Kumar, K., Singh, B. B., and Jain, V. K.: Distribution of  
568 VOCs in urban and rural atmospheres of subtropical India: Temporal variation, source  
569 attribution, ratios, OFP and risk assessment, *Science of the Total Environment*, 613-614,  
570 492-501, <https://doi.org/10.1016/j.scitotenv.2017.09.096>, 2018.

571 Lai, M., Zhang, D., Yin, S., Song, X., and Zhang, R.: Pollution characteristics,  
572 source apportionment and activity analysis of atmospheric VOCs during winter and  
573 summer pollution in Zhengzhou City, *Environmental Science*, 4108, 3500-3510,  
574 <https://doi.org/10.13227/j.hjcx.202001133>, 2024.

575 Li, B., Ho, S. S. H., Gong, S., Ni, J., Li, H., Han, L., Yang, Y., Qi, Y., and Zhao,  
576 D.: Characterization of VOCs and their related atmospheric processes in a central  
577 Chinese city during severe ozone pollution periods, *Atmospheric Chemistry and*  
578 *Physics*, 19, 617-638, <https://doi.org/10.5194/acp-19-617-2019>, 2019.

579 Li, J., Deng, S., Tohti, A., Li, G., Yi, X., Lu, Z., Liu, J., and Zhang, S.: Spatial  
580 characteristics of VOCs and their ozone and secondary organic aerosol formation  
581 potentials in autumn and winter in the Guanzhong Plain, China, *Environmental*  
582 *Research*, 211, 113036, <https://doi.org/10.1016/j.envres.2022.113036>, 2022.

583 Li, J., Xie, S. D., Zeng, L. M., Li, L. Y., Li, Y. Q., and Wu, R. R.: Characterization  
584 of ambient volatile organic compounds and their sources in Beijing, before, during, and  
585 after Asia-Pacific Economic Cooperation China 2014, *Atmospheric Chemistry and*  
586 *Physics*, 15, 7945-7959, <https://doi.org/10.5194/acp-15-7945-2015>, 2015.

587 Li, J., Lu, K., Lv, W., Li, J., Zhong, L., Ou, Y., Chen, D., Huang, X., and Zhang,  
588 Y.: Fast increasing of surface ozone concentrations in Pearl River Delta characterized  
589 by a regional air quality monitoring network during 2006–2011, *Journal of*  
590 *Environmental Sciences*, 26, 23-36, [https://doi.org/10.1016/S1001-0742\(13\)60377-0](https://doi.org/10.1016/S1001-0742(13)60377-0),  
591 2014.

592 Liu, Y., Li, X., Tang, G., Wang, L., Lv, B., Guo, X., and Wang, Y.: Secondary



593 organic aerosols in Jinan, an urban site in North China: Significant anthropogenic  
594 contributions to heavy pollution, *Journal of Environmental Sciences*, 80, 107-115,  
595 <https://doi.org/10.1016/j.jes.2018.11.009>, 2019.

596 Liu, Y., Shao, M., Fu, L., Lu, S., Zeng, L., and Tang, D.: Source profiles of volatile  
597 organic compounds (VOCs) measured in China: Part I, *Atmospheric Environment*, 42,  
598 6247-6260, <https://doi.org/10.1016/j.atmosenv.2008.01.070>, 2008.

599 Liu, Y., Song, M., Liu, X., Zhang, Y., Hui, L., Kong, L., Zhang, Y., Zhang, C., Qu,  
600 Y., An, J., Ma, D., Tan, Q., and Feng, M.: Characterization and sources of volatile  
601 organic compounds (VOCs) and their related changes during ozone pollution days in  
602 2016 in Beijing, China, *Environmental Pollution*, 257, 113599,  
603 <https://doi.org/10.1016/j.envpol.2019.113599>, 2020.

604 Liu, Z., Hu, K., Zhang, K., Zhu, S., Wang, M., and Li, L.: VOCs sources and roles  
605 in O<sub>3</sub> formation in the central Yangtze River Delta region of China, *Atmospheric*  
606 *Environment*, 302, <https://doi.org/10.1016/j.atmosenv.2023.119755>, 2023.

607 Li, X., Wang, S., Hao, J.: Characteristics of volatile organic compounds (VOCs)  
608 emitted from biofuel combustion in China, *Environmental Science*, 32, 3515-3521,  
609 2011.

610 Li, Y., Yin, S., Zhang R., Yu, S., Yang, J., and Zhang, D.: Characteristics and source  
611 apportionment of atmospheric VOCs at different pollution levels in winter in an urban  
612 area in Zhengzhou, *Environmental Science*, 4108, 3500-3510,  
613 <https://doi.org/10.13227/j.hjcx.202001133>, 2020.

614 Ma, Q., Wang, W., Wu, Y., Wang, F., Jin, L., Song, Y., Han, Y., Zhang, R., Zhang,  
615 D.: Haze caused by NO<sub>x</sub> oxidation under restricted residential and industrial activities  
616 in a mega city in the south of North China Plain, *Chemosphere*, Volume 305, 135489,  
617 <https://doi.org/10.1016/j.chemosphere.2022.135489>, 2022.

618 Merino, M., Marinescu, M., Cascajo, A., Carretero, J., Singh, D.: Evaluating the  
619 spread of Omicron COVID-19 variant in Spain, *Future Generation Computer Systems*,  
620 149, 547-561, <https://doi.org/10.1016/j.future.2023.07.025>, 2023.

621 Monod, A., Sive, B. C., Avino, P., Chen, T., Blake, D. R., and Sherwood Rowland,  
622 F.: Monoaromatic compounds in ambient air of various cities: a focus on correlations  
623 between the xylenes and ethylbenzene, *Atmospheric Environment*, 35, 135-149,  
624 [https://doi.org/10.1016/S1352-2310\(00\)00274-0](https://doi.org/10.1016/S1352-2310(00)00274-0), 2001.

625 Mozaffar, A., Zhang, Y.-L., Fan, M., Cao, F., and Lin, Y.-C.: Characteristics of  
626 summertime ambient VOCs and their contributions to O<sub>3</sub> and SOA formation in a

627 suburban area of Nanjing, China, *Atmospheric Research*, 240, 104923,  
628 <https://doi.org/10.1016/j.atmosres.2020.104923>, 2020.

629 Mu, L., Feng, C., Li, Y., Li, X., Liu, T., Jiang, X., Liu, Z., Bai, H., and Liu, X.:  
630 Emission factors and source profiles of VOCs emitted from coke production in Shanxi,  
631 China, *Environmental Pollution*, 335, 122373,  
632 <https://doi.org/10.1016/j.envpol.2023.122373>, 2023.

633 Niu, Y., Yan, Y., Chai, J., Zhang, X., Xu, Y., Duan, X., Wu, J., and Peng, L.: Effects  
634 of regional transport from different potential pollution areas on volatile organic  
635 compounds (VOCs) in Northern Beijing during non-heating and heating periods,  
636 *Science of the Total Environment*, 836, 155465,  
637 <https://doi.org/10.1016/j.scitotenv.2022.155465>, 2022.

638 Norris, G., Duvall, R., Brown, S., Bai, S. EPA Positive Matrix Factorization (PMF)  
639 5.0 Fundamentals and User Guide. U.S. Environmental Protection Agency, Washington,  
640 DC, EPA/600/R-14/108 (NTIS PB2015-105147), 2014.

641 Paatero, P., Eberly, S., Brown, S. G., Norris, G. A.: Methods for estimating  
642 uncertainty in factor analytic solutions, *Atmospheric Measurement Techniques*, Volume  
643 7, 781-797, <https://doi.org/10.5194/amt-7-781-2014>, 2014.

644 Pei, C., Yang, W., Zhang, Y., Song, W., Xiao, S., Wang, J., Zhang, J., Zhang, T.,  
645 Chen, D., Wang, Y., Chen, Y., Wang, X.: Decrease in ambient volatile organic  
646 compounds during the COVID-19 lockdown period in the Pearl River Delta region,  
647 south China, *Science of The Total Environment*, 823, 153720,  
648 <https://doi.org/10.1016/j.scitotenv.2022.153720>, 2022.

649 Petersen, M. S., Í Kongsstovu, S., Eliassen, E. H., Larsen, S., Hansen, J. L., Vest,  
650 N., Dahl, M. M., Christiansen, D. H., Møller, L. F., & Kristiansen, M. F.: Clinical  
651 characteristics of the Omicron variant - results from a Nationwide Symptoms Survey  
652 in the Faroe Islands, *International Journal of Infectious Diseases*, 122, 636–643,  
653 <https://doi.org/10.1016/j.ijid.2022.07.005>, 2022.

654 Qi, J., Mo, Z., Yuan, B., Huang, S., Huangfu, Y., Wang, Z., Li, X., Yang, S., Wang,  
655 W., Zhao, Y., Wang, X., Wang, W., Liu, K., and Shao, M.: An observation approach in  
656 evaluation of ozone production to precursor changes during the COVID-19 lockdown,  
657 *Atmospheric Environment*, 262, 118618,  
658 <https://doi.org/10.1016/j.atmosenv.2021.118618>, 2021.

659 Russo, R. S., Zhou, Y., White, M. L., Mao, H., Talbot, R., and Sive, B. C.: Multi-  
660 year (2004–2008) record of nonmethane hydrocarbons and halocarbons in New

661 England: seasonal variations and regional sources, *Atmospheric Chemistry and Physics*,  
662 10, 4909-4929, <https://doi.org/10.5194/acp-10-4909-2010>, 2010.

663 Sahu, L. K., Tripathi, N., Gupta, M., Singh, V., Yadav, R., Patel, K.: Impact of  
664 COVID-19 Pandemic lockdown in ambient concentrations of aromatic volatile organic  
665 compounds in a metropolitan city of western India, *Journal of geophysical research*,  
666 *Atmospheres : JGR*, 127(6), <https://doi.org/10.1029/2022JD036628>, 2022.

667 Schauer, J., Kleeman, M., Cass, G., Simoneit, B.: Measurement of emissions from  
668 air pollution sources.5. C<sub>1</sub>-C<sub>32</sub> organic compounds from gasoline-powered motor  
669 vehicles, *Environmental Science & Technology*, 36, 1169-1180,  
670 <https://doi.org/10.1021/es0108077>, 2002.

671 Shao, P., An, J., Xin, J., Wu, F., Wang, J., Ji, D., and Wang, Y.: Source  
672 apportionment of VOCs and the contribution to photochemical ozone formation during  
673 summer in the typical industrial area in the Yangtze River Delta, China, *Atmospheric*  
674 *Research*, 176-177, 64-74, <https://doi.org/10.1016/j.atmosres.2016.02.015>, 2016.

675 Shi, Y., Liu, C., Zhang, B., Simayi, M., Xi, Z., Ren, J., and Xie, S.: Accurate  
676 identification of key VOCs sources contributing to O<sub>3</sub> formation along the Liaodong  
677 Bay based on emission inventories and ambient observations, *Science of the Total*  
678 *Environment*, 844, 156998, [10.1016/j.scitotenv.2022.156998](https://doi.org/10.1016/j.scitotenv.2022.156998), 2022.

679 Singh, B., Sohrab, S., Athar, M., Alandijany, T., Kumari, S., Nair, A., Kumari, S.,  
680 Mehra, K., Chowdhary, K., Rahman, S., Azhar, E.: Substantial changes in selected  
681 volatile organic compounds (VOCs) and associations with health risk assessments in  
682 industrial areas during the COVID-19 Pandemic, *Toxics*, 11, 165,  
683 <https://doi.org/10.3390/toxics11020165>, 2023a.

684 Singh, B., Singh, M., Ulman, Y., Sharma, U., Pradhan, R., Sahoo, J., Padhi, S.,  
685 Chandra, P., Koul, M., Tripathi, P., Kumar, D., Masih, J.: Distribution and temporal  
686 variation of total volatile organic compounds concentrations associated with health risk  
687 in Punjab, India, *Case Studies in Chemical and Environmental Engineering*, 8, 100417,  
688 <https://doi.org/10.1016/j.cscee.2023.100417>, 2023b.

689 Song, M., Li, X., Yang, S., Yu, X., Zhou, S., Yang, Y., Chen, S., Dong, H., Liao,  
690 K., Chen, Q., Lu, K., Zhang, N., Cao, J., Zeng, L., and Zhang, Y.: Spatiotemporal  
691 variation, sources, and secondary transformation potential of volatile organic  
692 compounds in Xi'an, China, *Atmospheric Chemistry and Physics*, 21, 4939-4958,  
693 <https://doi.org/10.5194/acp-21-4939-2021>, 2021.

694 Song, X., Zhang, D., Li, X., Lu, X., Wang, M., Zhang, B., Zhang, R.: Simultaneous

695 observations of peroxyacetyl nitrate and ozone in Central China during static  
696 management of COVID-19: Regional transport and thermal decomposition,  
697 Atmospheric Research, Volume 294, 106958,  
698 <https://doi.org/10.1016/j.atmosres.2023.106958>, 2023.

699 Song, Y., Shao, M., Liu, Y., Lu, S., Kuster, W., Goldan, P., and Xie, S.: Source  
700 apportionment of ambient volatile organic compounds in Beijing, Environmental  
701 Science & Technology, 41, 4348-4353, <https://doi.org/10.1021/es0625982>, 2007.

702 Wang, H., Li, J., Peng, Y., Zhang, M., Che, H., Zhang, X.: The impacts of the  
703 meteorology features on PM<sub>2.5</sub> levels during a severe haze episode in central-east China,  
704 Atmospheric Environment, Volume 197, Pages 177-189, ISSN 1352-2310,  
705 <https://doi.org/10.1016/j.atmosenv.2018.10.001>, 2019.

706 Wang, H., Wang, Q., Chen, J. Chen, C., Huang, C., Qiao, L. Lou, S., Lu, J.: Do  
707 vehicular emissions dominate the source of C6–C8 aromatics in the megacity Shanghai  
708 of eastern China?, Environmental Science, 27, 290-297, <https://doi.org/10.1016/j.jes.2014.05.033>, 2015.

710 Wang, M., Lu, S., Shao, M., Zeng, L., Zheng, J., Xie, F., Lin, H., Hu, K., and Lu,  
711 X.: Impact of COVID-19 lockdown on ambient levels and sources of volatile organic  
712 compounds (VOCs) in Nanjing, China, Science of the Total Environment, 757, 143823,  
713 <https://doi.org/10.1016/j.scitotenv.2020.143823>, 2021.

714 Wang, M., Zeng, L., Lu, S., Shao, M., Liu, X., Yu, X., Chen, W., Yuan, B., Zhang,  
715 Q., Hu, M., & Zhang, Z.: Development and validation of a cryogen-free automatic gas  
716 chromatograph system (GC-MS/FID) for online measurements of volatile organic  
717 compounds, Analytical Methods, 6, 9424, <https://doi.org/10.1039/C4AY01855A>, 2014.

718 Wang, T., Xue, L., Brimblecombe, P., Lam, Y. F., Li, L., and Zhang, L.: Ozone  
719 pollution in China: A review of concentrations, meteorological influences, chemical  
720 precursors, and effects, Science of the Total Environment, 575, 1582-1596,  
721 <https://doi.org/10.1016/j.scitotenv.2016.10.081>, 2017.

722 Wu, R., Li, J., Hao, Y., Li, Y., Zeng, L., and Xie, S.: Evolution process and sources  
723 of ambient volatile organic compounds during a severe haze event in Beijing, China,  
724 Science of the Total Environment, 560-561, 62-72,  
725 <https://doi.org/10.1016/j.scitotenv.2016.04.030>, 2016.

726 Wu, W., Zhao, B., Wang, S., and Hao, J.: Ozone and secondary organic aerosol  
727 formation potential from anthropogenic volatile organic compounds emissions in China,  
728 Journal of Environmental Sciences, 53, 224-237,

729 <https://doi.org/10.1016/j.jes.2016.03.025>, 2017.

730 Xiong, Y., Zhou, J., Xing, Z., and Du, K.: Optimization of a volatile organic  
731 compound control strategy in an oil industry center in Canada by evaluating ozone and  
732 secondary organic aerosol formation potential, *Environmental Research*, 191, 110217,  
733 <https://doi.org/10.1016/j.envres.2020.110217>, 2020.

734 Yu, F., Wang, Q., Yan, Q., Jiang, N., Wei, J., Wei, Z., Yin, S.: Particle size  
735 distribution, chemical composition and meteorological factor analysis: A case study  
736 during wintertime snow cover in Zhengzhou, China, *Atmospheric Research*, 202, 140-  
737 147, 0169-8095, <https://doi.org/10.1016/j.atmosres.2017.11.016>, 2018.

738 Yun, L., Li, C., Zhang, M., He, L. and Guo, J.: Pollution characteristics and sources  
739 of atmospheric VOCs in the coastal background area of the Pearl River Delta,  
740 *Environmental Science*, 4191-4201, <https://doi.org/10.13227/j.hjkx.202101155>, 2021.

741 Zeng, X., Han, M., Ren, G., Liu, G., Wang, X., Du, K., Zhang, X., and Lin, H.: A  
742 comprehensive investigation on source apportionment and multi-directional regional  
743 transport of volatile organic compounds and ozone in urban Zhengzhou, *Chemosphere*,  
744 334, 139001, <https://doi.org/10.1016/j.chemosphere.2023.139001>, 2023.

745 Zhang, C., Liu, X., Zhang, Y., Tan, Q., Feng, M., Qu, Y., An, J., Deng, Y., Zhai, R.,  
746 Wang, Z., Cheng, N., and Zha, S.: Characteristics, source apportionment and chemical  
747 conversions of VOCs based on a comprehensive summer observation experiment in  
748 Beijing, *Atmospheric Pollution Research*, 12, 230-241,  
749 <https://doi.org/10.1016/j.apr.2020.12.010>, 2021a.

750 Zhang, D., He, B., Yuan, M., Yu, S., Yin, S., and Zhang, R.: Characteristics,  
751 sources and health risks assessment of VOCs in Zhengzhou, China during haze  
752 pollution season, *Journal of Environmental Sciences*, 108, 44-57,  
753 <https://doi.org/10.1016/j.jes.2021.01.035>, 2021b.

754 Zhang, D., Li, X., Yuan, M., Xu, Y., Xu, Q., Su, F., Wang, S., Zhang, R.:  
755 Characteristics and sources of nonmethane volatile organic compounds (NMVOCs) and  
756 O<sub>3</sub>-NO<sub>x</sub>-NMVOC relationships in Zhengzhou, China, *Atmosphere Chemistry and  
757 Physics*, 24, 8549-8567, <https://doi.org/10.5194/acp-24-8549-2024>, 2024.

758 Zhang, F., Shang, X., Chen, H., Xie, G., Fu, Y., Wu, D., Sun, W., Liu, P., Zhang,  
759 C., Mu, Y., Zeng, L., Wan, M., Wang, Y., Xiao, H., Wang, G., and Chen, J.: Significant  
760 impact of coal combustion on VOCs emissions in winter in a North China rural site,  
761 *Science of the Total Environment*, 720, 137617,  
762 <https://doi.org/10.1016/j.scitotenv.2020.137617>, 2020.

763 Zhang, J., Sun, Y., Wu, F., Sun, J., and Wang, Y.: The characteristics, seasonal  
764 variation and source apportionment of VOCs at Gongga Mountain, China, *Atmospheric*  
765 *Environment*, 88, 297-305, <https://doi.org/10.1016/j.atmosenv.2013.03.036>, 2014.

766 Zhang, Z., Yan, X., Gao, F., Thai, P., Wang, H., Chen, D., Zhou, L., Gong, D., Li,  
767 Q., Morawska, L., and Wang, B.: Emission and health risk assessment of volatile  
768 organic compounds in various processes of a petroleum refinery in the Pearl River Delta,  
769 China, *Environmental Pollution*, 238, 452-461,  
770 <https://doi.org/10.1016/j.envpol.2018.03.054>, 2018.

771 Zheng, H., Kong, S., Xing, X., Mao, Y., Hu, T., Ding, Y., Li, G., Liu, D., Li, S.,  
772 and Qi, S.: Monitoring of volatile organic compounds (VOCs) from an oil and gas  
773 station in northwest China for 1 year, *Atmospheric Chemistry and Physics*, 18, 4567-  
774 4595, <https://doi.org/10.5194/acp-18-4567-2018>, 2018.

775 Zheng, J., Zhong, L., Wang, T., Louie, P. K. K., and Li, Z.: Ground-level ozone in  
776 the Pearl River Delta region: Analysis of data from a recently established regional air  
777 quality monitoring network, *Atmospheric Environment*, 44, 814-823,  
778 <https://doi.org/10.1016/j.atmosenv.2009.11.032>, 2010.

779 Zhou, Z., Xiao, L., Fei, L., Yu, W., Lin M., Huang, T., Zhang, Z. and Tao J.:  
780 Characteristics and sources of VOCs during ozone pollution and non-pollution periods  
781 in summer in Dongguan industrial concentration area, *Environmental Science*, 4497-  
782 4505, <https://doi.org/10.13227/j.hjcx.202111285>, 2022.

783 Zou, Y., Yan, X. L., Flores, R. M., Zhang, L. Y., Yang, S. P., Fan, L. Y., Deng, T.,  
784 Deng, X. J., and Ye, D. Q.: Source apportionment and ozone formation mechanism of  
785 VOCs considering photochemical loss in Guangzhou, China, *Science of the Total*  
786 *Environment*, 903, 166191, <https://doi.org/10.1016/j.scitotenv.2023.166191>, 2023.

787 Zuo, H., Jiang, Y., Yuan, J., Wang, Z., Zhang, P., Guo, C., Wang, Z., Chen, Y., Wen,  
788 Q., Wei, Y., Li, X.: Pollution characteristics and source differences of VOCs before and  
789 after COVID-19 in Beijing, *Science of The Total Environment*, 907, 167694,  
790 <https://doi.org/10.1016/j.scitotenv.2023.167694>, 2024.

791